Chaos, Solitons and Fractals 136 (2020) 109790

Contents lists available at ScienceDirect

Chaos, Solitons and Fractals

Nonlinear Science, and Nonequilibrium and Complex Phenomena

journal homepage: www.elsevier.com/locate/chaos

Influence of numerical noises on computer-generated simulation of spatio-temporal chaos

Shijie Qin[a], Shijun Liao[a,b,c,d,*]

[a] State Key Laboratory of Ocean Engineering, Shanghai 200240, China
[b] Center of Advanced Computing, School of Naval Architecture, Ocean and Civil Engineering, Shanghai Jiaotong University, Shanghai 200240, China
[c] State Key Laboratory of Plateau Ecology and Agriculture, Xining 810018, China
[d] School of Hydraulic and Electric Engineering, Qinghai University, Xining 810018, China

ARTICLE INFO

Article history:
Received 24 January 2020
Revised 29 March 2020
Accepted 1 April 2020
Available online 14 April 2020

MSC:
37D45
34C28
65P20
65M12

Keywords:
Spatio-temporal chaos
Numerical noises
Reliability

ABSTRACT

Due to the famous butterfly-effect, it is rather difficult to gain a reliable simulation of chaos in an interval of time that is long enough from statistic viewpoint. In this paper we propose an efficient numerical strategy of the clean numerical simulation (CNS) in physical space to gain reliable simulation of spatio-temporal chaos in a long enough interval of time by means of reducing both of truncation and round-off error to a required tiny level. Without loss of generality, the damped driven sine-Gordon equation is used to illustrate its validity for spatio-temporal chaos. The reliable result in a long interval of time given by this CNS algorithm is used as benchmark solution to investigate the influence of numerical noise (i.e. truncation and round-off error) by comparing it in details with those given by the Runge-Kutta's method in double precision. It is found that numerical noise can lead to, both quantitatively and qualitatively, huge deviation of the spatio-temporal chaotic system not only in trajectories but also even in *statistics*! Therefore, in practice we should check very carefully the reliability of computer-generated simulations of spatio-temporal chaotic systems (including turbulent flows), especially when the duration of simulation is quite long. The new strategy of the CNS in physical space provides us an efficient way to accurately study lots of spatio-temporal chaotic systems in science and engineering in a long enough interval of time so as to reveal some new physical truths by means of clearing away numerical noises.

© 2020 Elsevier Ltd. All rights reserved.

1. Introduction

Plenty of complicated problems in science, finance and engineering have been solved with satisfied precision by means of high performance digit computers. However, even using the most advanced computers, some problems such as chaotic dynamical systems [1–6], are still rather difficult to solve.

It is well known that all numerical simulations are not "clean": more or less numerical noises (i.e. truncation error and round-off error) always exist, which depend on numerical algorithms and data precision, respectively. In many cases, such kind of numerical noises can be controlled to such a tiny level (much smaller than variables under investigation) that their influence can be almost neglected. However, numerical noises increase exponentially for chaotic dynamic systems due to the sensitive dependence on initial conditions (SDIC), which was first discovered by Poincaré [7] in 1890 and rediscovered by Lorenz [8] in 1963 with a more famous name "butterfly effect". Thus, for a chaotic dynamic system, a very tiny variation of initial condition may bring a huge difference of numerical simulations after a long enough time [5,9]. Furthermore, as reported by Lorenz [10] a chaotic system is sensitive *not only* to initial condition *but also* to numerical algorithm: the (maximum) Lyapunov exponent of a chaotic model always alters between negative and positive values even when the time-step becomes rather small. Teixeira et al. [11] further investigated the time step sensitivity of three nonlinear atmospheric models by means of traditional algorithms in *double* precision, and made a rather pessimistic conclusion that "for chaotic systems, numerical convergence cannot be guaranteed *forever*".

Certainly, the reliability of computer-generated simulation of chaotic systems is a fundamental problem. Anosov [12] and Bowen [13] proved that *uniformly hyperbolic* systems have the so-called shadowing property, say, a computer-generated (or noisy) orbit will stay close to (shadow) true orbits with *adjusted* initial conditions for arbitrarily long times [12–17]. However, it is a pity that *hardly* any of chaotic systems is uniformly hyperbolic. Daw-

* Corresponding author at: Shanghai Jiaotong University, 800 Dongchuan Rd, Shanghai 200240, China.
E-mail address: sjliao@sjtu.edu.cn (S. Liao).

https://doi.org/10.1016/j.chaos.2020.109790
0960-0779/© 2020 Elsevier Ltd. All rights reserved.

son et al. [18] showed that the non-existence of such shadowing trajectories may be caused by finite-time Lyapunov exponents of a system fluctuating about zero. For the non-hyperbolic chaotic systems with unstable dimension variability, no true trajectory of reasonable length can be found to exist near any numerical trajectories [19]. It was found [20] that extremely small numerical noises might result in macroscopic errors even in simulation average *statistics* that are several orders of magnitude larger than the noise level. Thus, the good promise from the Shadow Lemma [12,13] for a uniformly hyperbolic system does not work on many non-hyperbolic systems [21]. It seems that we had to be satisfied with finite-length shadows for non-hyperbolic systems [22]. Note that most of investigations on shadows are based on low dimensional dynamic systems, although a shadowing algorithm for high dimensional systems was proposed [22]. To the best of our knowledge, neither rigorous shadowing theorems nor practical shadowing algorithms have been proposed for spatio-temporal chaotic systems governed by nonlinear PDEs with an infinite number of dimensions. It seems that, although the shadowing concept is rigorous in mathematics, it is hardly used in practice for non-hyperbolic spatio-temporal chaotic systems that widely exist.

To overcome the above-mentioned limitations of traditional algorithms in *double* precision, Liao [23] suggested a numerical strategy in 2009, namely the "Clean Numerical Simulation" (CNS) [24,25]. By means of the CNS, reliable/convergent numerical simulations of chaotic dynamical systems can be obtained in a controllable interval of time $0 \le t \le T_c$, where T_c is called "critical predictable time". The CNS is based on the high-order Taylor expansion method [26]

$$f(t+\Delta t) = f(t) + \sum_{m=1}^{M} \frac{1}{m!} \frac{d^m f(t)}{dt^m} (\Delta t)^m, \tag{1}$$

where f is a function, t and Δt denote the time and time-step, respectively, which is adopted to decrease the truncation error to a required level by means of a large enough order M, and the use of the multiple precision (MP, called the MPFR library in the C language) [27], which is adopted to decrease the round-off error to a required level via reserving a large enough number N_s of significant digit for *all* physical/numerical variables and parameters. Besides, an additional simulation with even smaller numerical noises is necessary to determine the critical predictable time T_c by comparing these two simulations with each other, as mentioned below.

The CNS is based on such a hypothesis that the level of numerical noises increases exponentially (in an average meaning) within an interval of time $t \in [0, T_c]$, i.e.

$$\mathcal{E}(t) = \mathcal{E}_0 \exp(\kappa t), \qquad t \in [0, T_c], \tag{2}$$

where the constant $\kappa > 0$ is called noise-growing exponent, $\mathcal{E}_0$ denotes the level of initial noises (i.e. truncation and round-off error), and $\mathcal{E}(t)$ is the level of evolving noises of numerical simulation, respectively. In theory, the critical predictable time T_c is governed by a critical level of noise $\mathcal{E}_c$, say,

$$\mathcal{E}_c = \mathcal{E}_0 \exp(\kappa T_c). \tag{3}$$

Obviously, for a fixed value of $\mathcal{E}_c$, the smaller the initial noise $\mathcal{E}_0$, the larger the critical predictable time T_c.

However, it is practically impossible to exactly calculate the evolving noise $\mathcal{E}(t)$, because we do not known the true solution. So, we need a practical method with satisfied accuracy to determine T_c. Let $\mathbf{x} \in \Omega$ denote a vector of spatial coordinates, $\phi(\mathbf{x}, t)$ be a numerical simulation reliable in $t \in [0, T_c]$ with initial noise $\mathcal{E}_0$, and $\phi'(\mathbf{x}, t)$ be another simulation (with the same physical parameters and the same initial/boundary conditions) in $t \in [0, T_c']$ with the initial noise $\mathcal{E}_0'$ that is several orders of magnitude smaller than $\mathcal{E}_0$. According to the hypothesis of exponential growing of numerical noise of chaotic systems, it holds $T_c' > T_c$ and $\phi'(\mathbf{x}, t)$ in $t \in [0, T_c]$ should be much closer to the true solution than $\phi(\mathbf{x}, t)$. Therefore, $\phi'(\mathbf{x}, t)$ can be regarded as a *benchmark* solution to approximately calculate the noise of $\phi(\mathbf{x}, t)$ in $\mathbf{x} \in \Omega$. So, in practice, T_c is determined by comparing $\phi(\mathbf{x}, t)$ with a better simulation $\phi'(\mathbf{x}, t)$ having smaller noise $\mathcal{E}_0'$. In this way, the numerical noise of $\phi(\mathbf{x}, t)$ is guaranteed below the critical level $\mathcal{E}_c$ of noise in the temporal interval $t \in [0, T_c]$ within the whole spatial domain $\mathbf{x} \in \mathbf{\Omega}$. In other words, $\phi(\mathbf{x}, t)$ is a "clean" numerical simulation (CNS) in $t \in [0, T_c]$ and $\mathbf{x} \in \mathbf{\Omega}$. This provides us a heuristic explanation of the strategy of the CNS. Note that the CNS works even for non-pyherbolic systems and thus is more general than the shadowing theorem [12–17].

The CNS has been successfully used to gain reliable computer-generated simulations of many chaotic systems. For example, using traditional numerical algorithms in *double* precision, one often gains reliable/convergent numerical simulations of chaotic solution of Lorenz equation in a rather short interval, say, approximately [0, 32]. However, by means of the CNS, a convergent and reliable numerical simulation of the chaotic solution of Lorenz equations in a rather long interval $[0, 10, 000]$ was obtained for the first time [28]. Besides, numerical noises of the CNS can be much smaller even than micro-level physical uncertainty so that, via the CNS, one can provide a rigorous theoretical evidence that the micro-level physical thermal fluctuation is the origin of the macroscopic randomness of Rayleigh–Bénard turbulent flows [29]. In addition, the CNS has been successfully adopted to find more than 2000 new periodic orbits of three-body system [30–32]. The discovery of these new periodic orbits were reported twice by New Scientist [33,34], because only three families of periodic orbits of three-body problem were reported in three hundred years after Newton mentioned this famous problem! All of these illustrate the validity and potential of the CNS for complicated nonlinear problems.

A spatio-temporal chaos has an infinite number of dimensions in principle, and thus is more difficult to solve than a temporal chaos. It is worth noting that, the spatio-temporal chaos may have a close relationship with turbulence [35]. For the two-dimensional Rayleigh–Bénard turbulent flows described by the Navier–Stokes equations, the Galerkin–Fourier spectral method is used in the frame of the CNS, which is however rather time-consuming [29]. In this manuscript, we propose a new strategy of the CNS in physical space for spatio-temporal chaotic dynamic systems so as to greatly increase the computational efficiency. Then, using the reliable simulation given by the CNS as a benchmark solution, we further investigate the influence of the numerical noises on simulations of spatio-temporal chaos gained by the traditional algorithms in *double* precision. Using the sine-Gordon equation [36] as an example, we illustrate that numerical noises can lead to great deviations not only in spatio-temporal trajectories but also even in *statistics* for spatio-temporal chaos! The new strategy of the CNS in physical space provides us an efficient way to more accurately study lots of spatio-temporal chaotic systems in science and engineering in a long enough interval of time so as to reveal some new physical truths by means of clearing away numerical noises.

2. Mathematical model

Without loss of generality, let us consider the continuum limit of a chain of pendulums coupled through elastic restoring force and damped friction (see Fig. 1), governed by the damped driven sine-Gordon equation [36–38]:

$$u_{tt} = u_{xx} - \sin(u) - \alpha u_t + \Gamma \sin(\omega t - \lambda x) \tag{4}$$

with a periodic boundary condition

$$u(x + l, t) = u(x, t), \tag{5}$$

where u denotes the angle corresponding to the vertical direction of the pendulum, t and x are the temporal and spatial variables, the

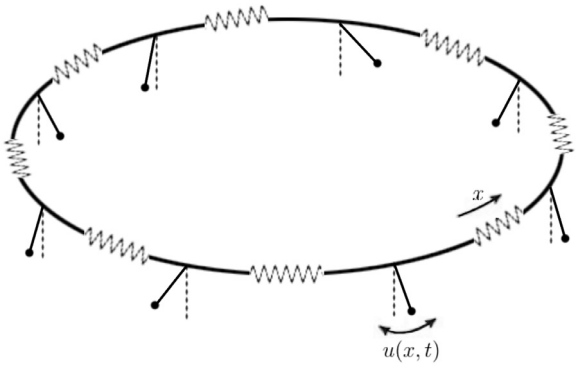

Fig. 1. A periodic pendulum chain.

subscript denotes the derivative, α and Γ are physical parameters, ω is the temporal frequency, $\lambda = 2\pi/l$ and l is the total length of the system, respectively. Using the transformation $x' = \lambda x + \pi$, the governing equation becomes

$$u_{tt} = \lambda^2 u_{xx} - \sin(u) - \alpha u_t - \Gamma \sin(\omega t - x), \tag{6}$$

where $t > 0$, $x \in [0, 2\pi]$, and the prime is neglected.

Without loss of generality, let us follow Chacón et al. [36] to choose the physical parameters

$$\omega = \frac{3}{5}, \quad \alpha = \frac{1}{10}, \quad \Gamma = \frac{461}{500}, \quad l = 500, \quad \lambda = \frac{2\pi}{l} = \frac{\pi}{250} \tag{7}$$

with the zero initial condition

$$u(x, 0) = 0, \qquad u_t(x, 0) = 0, \tag{8}$$

corresponding to a spatio-temporal chaos. This model is used in the following sections to describe the basic ideas and illustrate the validity of the new strategy of the CNS.

3. Numerical algorithm for spatio-temporal chaos

Lin et al. [29] combined the CNS with the Galerkin–Fourier spectral method to solve a two-dimensional Rayleigh–Bénard turbulent flows by mapping the original nonlinear PDE in physical space onto a huge system of nonlinear ODEs in spectral space. However, this approach is rather time-consuming [29] and impractical on present-day computers for simulation of spatio-temporal chaos. Here, we propose a much more efficient algorithm of the CNS in physical space for spatio-temporal chaos.

3.1. An efficient algorithm of the CNS in physical space

Here the basic ideas of the CNS algorithm in physical space is described by using the damped driven sine-Gordon Eq. (4) as an example. First, the spatial interval $x \in [0, 2\pi]$ is discretized by N equidistant points, say,

$$x_k = \frac{2\pi k}{N}, \tag{9}$$

where $k = 0, 1, 2, \ldots, N-1$ and x_k denotes different points in the physical space. In other words, the unknown continuous function $u(x, t)$ is approximated by a set of N discretized variables

$$\mathcal{S}(t) = \Big\{ u(x_0, t), u(x_1, t), u(x_2, t), \cdots, u(x_{N-1}, t) \Big\}.$$

In the temporal dimension, the high-order Taylor expansion method

$$u(x_k, t + \Delta t) \approx u(x_k, t) + \sum_{m=1}^{M} u^{[m]}(x_k, t)(\Delta t)^m \tag{10}$$

is used, where Δt is time-step and

$$u^{[m]}(x_k, t) = \frac{1}{m!} \frac{\partial^m u(x_k, t)}{\partial t^m}. \tag{11}$$

Here, for a given time-step Δt, the order M should be large enough so as to reduce the truncation error (in the temporal dimension) to a required tiny level. Besides, *all* physical/numerical variables and parameters must be in the multiple precision with a large enough number of significant digits so as to reduce the round-off error to a required tiny level. Note that from Eq. (10) we have

$$u^{[1]}(x_k, t + \Delta t) \approx u^{[1]}(x_k, t) + \sum_{m=1}^{M} (m+1) u^{[m+1]}(x_k, t)(\Delta t)^m. \tag{12}$$

Differentiating both sides of Eq. (6) $(m-2)$ times with respect to t and then dividing them by $m!$, we obtain the high-order temporal derivatives

$$\begin{aligned} u^{[m]}(x_k, t) = & \frac{1}{(m-1)m} \Big[\lambda^2 u_{xx}^{[m-2]}(x_k, t) - W_{m-2}(x_k, t) \Big] \\ & - \left(\frac{\alpha}{m} \right) u^{[m-1]}(x_k, t) - \left(\frac{\Gamma \omega^{m-2}}{m!} \right) F_{m-2}(x_k, t) \end{aligned} \tag{13}$$

for arbitrary $m \geq 2$, where

$$F_s(x_k, t) = \begin{cases} +\sin(\omega t - x_k), & s = 4r, \\ +\cos(\omega t - x_k), & s = 4r+1, \\ -\sin(\omega t - x_k), & s = 4r+2, \\ -\cos(\omega t - x_k), & s = 4r+3 \end{cases} \tag{14}$$

for an integer $r \geq 0$ and

$$W_{m-2}(x_k, t) = \frac{1}{(m-2)!} \frac{\partial^{m-2} \sin u(x_k, t)}{\partial t^{m-2}} \tag{15}$$

is given by the following recursion formulas

$$\begin{aligned} W_0(x_k, t) &= \sin u(x_k, t), \\ V_0(x_k, t) &= \cos u(x_k, t), \\ W_j(x_k, t) &= \frac{1}{j} \sum_{i=0}^{j-1} (j-i) u^{[j-i]}(x_k, t) V_i(x_k, t), \qquad j \geq 1, \\ V_j(x_k, t) &= -\frac{1}{j} \sum_{i=0}^{j-1} (j-i) u^{[j-i]}(x_k, t) W_i(x_k, t), \qquad j \geq 1. \end{aligned}$$

However, for spatio-temporal chaos, there always exist some terms with spatial derivative, such as $u_{xx}^{[m-2]}(x_k, t)$ in Eq. (13). Although $u^{[m-2]}(x_k, t)$ can be obtained by means of either Eqs. (10) or (12) or (13) with high accuracy, its spatial derivative $u_{xx}^{[m-2]}(x_k, t)$ is still unknown, which must be gained with a high accuracy, too. In theory, one of the most accurate approximations of the spatial derivative of $u^{[j]}(x, t)$ is its Fourier spectral expression, i.e.

$$\begin{aligned} u^{[j]}(x, t) \approx & \frac{1}{2} a_{j,0}(t) + \sum_{n=1}^{\frac{N}{2}-1} \Big[a_{j,n}(t) \cos(nx) + b_{j,n}(t) \sin(nx) \Big] \\ & + a_{j,\frac{N}{2}}(t) \cos\left(\frac{Nx}{2} \right), \end{aligned} \tag{16}$$

where

$$a_{j,n}(t) = \frac{2}{N} \sum_{k=0}^{N-1} u^{[j]}(x_k, t) \cos(nx_k), \tag{17}$$

$$b_{j,n}(t) = \frac{2}{N} \sum_{k=0}^{N-1} u^{[j]}(x_k, t) \sin(nx_k). \tag{18}$$

Here, the fast Fourier transform (FFT) algorithm is used. Then, we can obtain a rather accurate approximation of $u_{xx}^{[j]}(x_k, t)$ by means of (16), where $k = 0, 1, 2, \ldots, N-1$ and $j \geq 0$, as long as the mode number N is large enough so that the spatial truncation error can be decreased to a required tiny level.

Note that, if the order M of the Taylor expansion (10) is large enough, the *temporal* truncation error can be controlled below a required tiny level. Besides, if the spatial discretization is fine enough, say, the mode number N is large enough, the *spatial* truncation error in the Fourier spectral expression (16) and besides the corresponding spatial derivative term $u_{xx}^{[m-2]}(x_k, t)$ in Eq. (13) can be reduced to a required tiny level. In addition, all physical/numerical variables and parameters are expressed in multiple precision with a large enough number N_s of significant digits so that the round-off error can be controlled below a required tiny level. In this way, both of the round-off error and *spatio-temporal* truncation error can be controlled below a required tiny level.

In practice, in order to gain reliable simulations more efficiently, the variable stepsize (VS) scheme [39] is applied in the temporal dimension with a given allowed tolerance *tol* of the governing equations, since the high-order Taylor expansion method with the VS scheme is more efficient for high precision calculation. According to Barrio et al. [39], the optimal time stepsize is determined by

$$\Delta t = min\left(\frac{g(tol, M-1)}{\|u^{[M-1]}(x_k, t)\|_\infty^{\frac{1}{M-1}}}, \frac{g(tol, M)}{\|u^{[M]}(x_k, t)\|_\infty^{\frac{1}{M}}} \right), \tag{19}$$

where $\| \ \|_\infty$ is the infinite norm, *tol* is the allowed tolerance and

$$g(tol, M) \approx tol^{\frac{1}{M+1}}. \tag{20}$$

Thus, for a given *tol*, one has some freedom to choose a proper value of M for a high computational efficiency. In this paper, we adopt the following empirical formula

$$M = -\log(tol) - 10. \tag{21}$$

Besides, since the round-off error should be in the same level of the (temporal) truncation error, we have

$$tol = 10^{-N_s}, \tag{22}$$

where N_s is the number of significant digits for all physical/numerical variables and parameters in multiple precision. In this way, instead of choosing the order M of the truncated Taylor expansion or the time stepsize Δt, we can control the spatial and temporal truncation errors by choosing a large enough mode number N of the spatial Fourier expansion (16) and a large enough number of significant digits for multiple precision, which via (22) corresponds to a small enough temporal allowed tolerance *tol* of the governing equations by means of the VS scheme [39], respectively.

As reported by Lin *et al* [29], it is time-consuming to calculate the high-order derivatives of nonlinear terms in governing equation with respect to time by means of the CNS algorithm in spectral space. This restriction can be overcome by means of the above-mentioned CNS algorithm in physical space, as illustrated below.

3.2. Criteria of convergence and reliability

In the frame of the CNS, an additional simulation with smaller numerical noises is required to determine the "critical predictable time" T_c by comparing them with each other, so that both of them should have no distinct differences in the time interval $0 \leq t \leq T_c$ within the whole spatial domain $\mathbf{x} \in \Omega$.

How to compare two numerical simulations of a spatio-temporal chaotic system at a given time? Let $u(x, t)$ (with the mode-number N of spatial Fourier expansion) and $u'(x, t)$ (with the mode-number N' of the spatial Fourier expansion) denote two simulations with different levels of numerical noises, where $N' \geq N$ and $u'(x, t)$ has smaller numerical noises than $u(x, t)$. According to the hypothesis that numerical noise increases exponentially so that chaotic trajectory departs from its true solution very quickly, we can use $u'(x, t)$ as a benchmark solution to check the reliability of $u(x, t)$ in a limited interval of time. At a given time t, each of them can be expressed by the spatial Fourier expansion (16), with $a_{0,n}$, $b_{0,n}$, $a'_{0,n}$ and $b'_{0,n}$ denoting the corresponding coefficients. Write

$$c_n^2 = a_{0,n}^2 + b_{0,n}^2, \qquad (c'_n)^2 = (a'_{0,n})^2 + (b'_{0,n})^2. \tag{23}$$

Let us define

$$\delta_s(t) = \frac{\sum_{n=0}^{\frac{N}{2}} \left| (c'_n)^2 - c_n^2 \right|}{\sum_{n=0}^{\frac{N'}{2}} (c'_n)^2}, \tag{24}$$

called "the spectrum-deviation", to measure the deviation of $u(x, t)$ from the benchmark solution $u'(x, t)$. Then, the critical predictable time T_c of the simulation $u(x, t)$ (with the larger numerical noise) is determined by the criteria

$$\delta_s(t) \leq \delta_s^c, \tag{25}$$

where $\delta_s^c > 0$ is a small constant. It is found that $\delta_s^c = 1\%$ is good enough in practice. For example, let us choose the temporal allowed tolerance $tol = 10^{-60}$, corresponding to $N_s = 60$ by means of (22). Two numerical simulations are given by the above-mentioned CNS algorithm using $N = 8192$ and $N = 16384$ in the spatial discretization and the same precision (i.e. $N_s = 60$), respectively. Obviously, the CNS result given by $N = 8192$ has larger numerical noise than the CNS result given by $N = 16384$ so that the latter can be regarded as a benchmark solution of the former. Its spectrum-deviation δ_s (of the CNS result given by $N = 8192$) versus the time is as shown in Fig. 2(a). Using the criteria (25), we gain its corresponding "critical predictable time" $T_c \approx 465$. Note that the two CNS results have no distinct difference even at $t = 500$, as shown in Fig. 2(b), so that T_c determined by the criteria (25) is underestimated in practice. This however guarantees the reliability/convergence of our CNS result (given by $N = 8192$) in $[0, T_c]$, where $T_c \approx 465$. Thus, we use $\delta_s^c = 1\%$ as the reliability criteria to determine the critical predictable time T_c thereafter.

Using the temporal allowed tolerance $tol = 10^{-60}$ (and $N_s = 60$) for the multiple precision, it is found that the critical predictable time T_c increases almost linearly with respect to the mode number N of the spatial Fourier expansion, say,

$$T_c \approx 0.0558N + 10.7, \tag{26}$$

as shown in Fig. 3. Besides, if N is large enough, for example $N = 16384$, and *tol* is given by (22), it is found that the critical predictable time T_c increases almost linearly with respect to N_s, say,

$$T_c \approx 16.5N_s - 87.8, \tag{27}$$

as shown in Fig. 4, where N_s is the number of significant digits for multiple precision. Notably, when $N_s = 16$, corresponding to the double precision, one has $T_c \approx 175$, say, using the double precision one can gain a reliable computer-generated simulation at most in $t \leq 175$, even if truncation error is very small by using a rather high order of temporal Taylor expansion and a rather large mode number N of the spatial Fourier expansion. This is exactly the same reason why high-order algorithms in double precision are useless for modifying convergence of chaotic computer-generated results, as previously mentioned by many researchers [8,10,11].

From (26) and (27), we have the linear relationship

$$T_c \approx \min\left\{0.0558N + 10.7, 16.5N_s - 87.8\right\}. \tag{28}$$

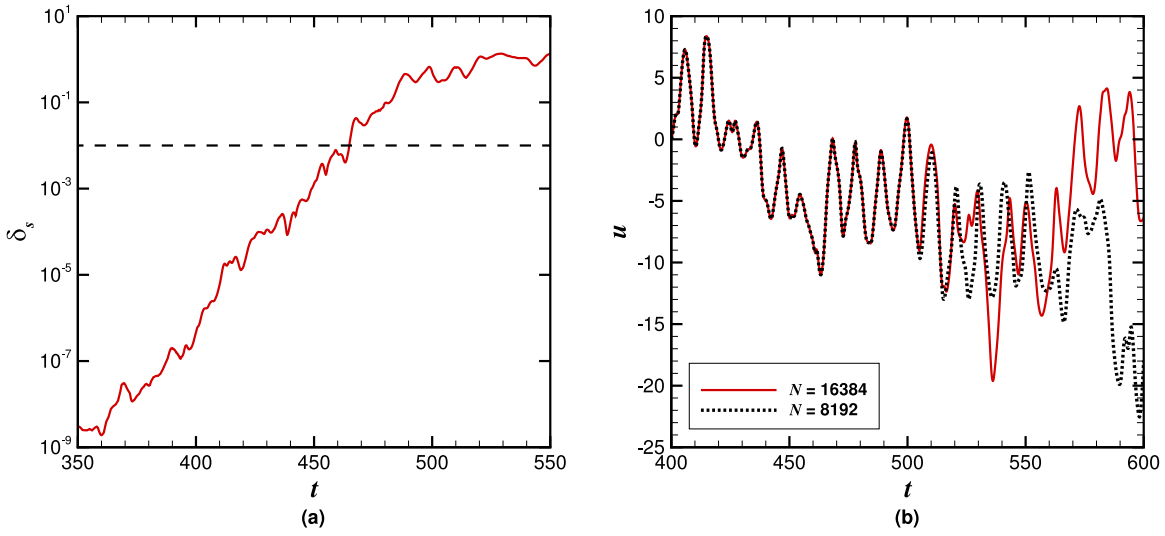

Fig. 2. The spectrum-deviation $\delta_s(t)$ of $u(x, t)$ and the comparison of $u(x, t)$ at $x = 0$, given by the two CNS results using the same temporal allowed tolerance $tol = 10^{-60}$ and the same number $N_s = 60$ of the significant digits in multiple precision, but using two different mode-numbers $N = 8192$ and $N = 16384$ of the spatial Fourier expansion, respectively. (a) The spectrum-deviation $\delta_s(t)$, where the dashed line corresponds to $\delta_s = 1\%$; (b) Comparison of the two CNS results at $x = 0$.

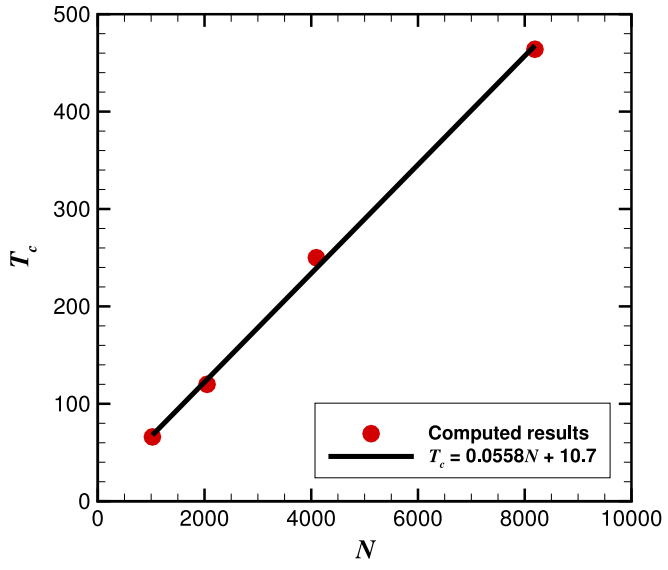

Fig. 3. The critical predictable time T_c versus the mode-number N of the spatial Fourier expansion, given by means of the temporal allowed tolerance $tol = 10^{-60}$ in a VS scheme and the number $N_s = 70$ of significant digits in multiple precision.

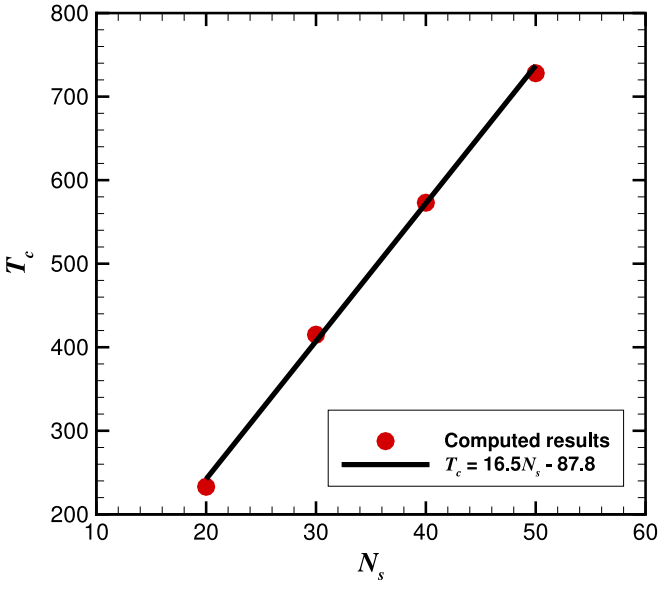

Fig. 4. The critical predictable time T_c versus the significant digit number N_s in multiple precision, given by means of the mode-number $N = 16384$ of the spatial Fourier expansion and the temporal allowed tolerance *tol* via (22).

Thus, for a given critical predictable time T_c, we can always find the corresponding mode-number N of the spatial Fourier expansion by means of (26), and the significant digit number N_s of multiple precision by means of (27) that further determines the temporal allowed tolerance *tol* via (22), respectively, so as to gain a reliable chaotic solution in $0 \le t \le T_c$ within the whole spatial domain $x \in [0, 2\pi]$. For example, if we would like to give a reliable chaotic solution (of the considered problem) with the critical predictable time $T_c = 900$, we should use $N = 16384$, $tol = 10^{-60}$ and $N_s = 60$. Therefore, the above formula is important in practice, especially for a quite large T_c.

4. Influence of numerical noises on chaotic results

Due to the butterfly-effect, hardly one can gain a reliable computer-generated simulation of chaos in a long enough interval of time. Even so, it is however widely believed that one might gain satisfied result of chaos in *statistics*, although trajectory given by traditional algorithms often departs rather quickly from true solution. Is this indeed true? This is a fundamental problem for spatio-temporal chaos. In this section, we use the sine-Gordon equation to illustrate that the above speculation is wrong for the considered chaotic case: numerical noises might lead to huge deviations of chaos not only in trajectory but also even in *statistics*!

From viewpoint of statistics for a spatio-temporal chaos, the time duration of computer-generated simulation should be long enough. According to (26) and (27), we can gain a reliable/convergent simulation of the spatio-temporal chaos in a long enough interval of time $t \in [0, 900]$ by means of the CNS algorithm (in physical space) using the mode number $N = 16384$ of the spatial Fourier expansion, the temporal allowed tolerance $tol = 10^{-60}$ for the high-order Taylor expansion and the significant digit number $N_s = 60$ in multiple precision for all physical/numerical vari-

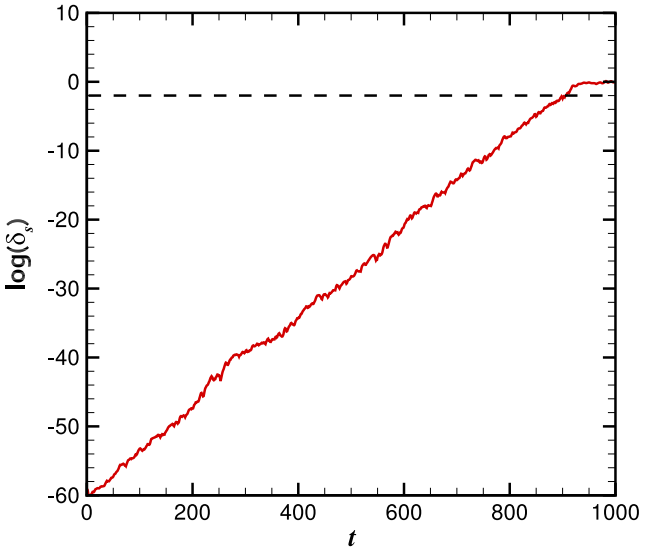

Fig. 5. Spectrum-deviation $\delta_s(t)$ of the CNS result given by $N = 16384$, $tol = 10^{-60}$ and $N_s = 60$. Dashed line: $\delta_s = 1\%$.

ables and parameters. To double-check the reliability of this CNS result once again, we compare it with another CNS result having even *smaller* numerical noises, given by the same mode number $N = 16384$ but a *smaller* temporal allowed tolerance $tol = 10^{-70}$ and a *higher* multiple precision with more significant digits, say, $N_s = 70$. Note that the corresponding spectrum-deviation δ_s of the two CNS results is indeed less than 1% in $0 \le t \le 900$, as shown in Fig. 5. This verifies the reliability of the CNS result given by means of $N = 16384$, $tol = 10^{-60}$ and $N_s = 60$, which is therefore used in the following parts as a benchmark solution for the comparisons with the simulations given by traditional numerical algorithms in *double* precision.

To investigate the influence of numerical noises, the same governing equation with the same initial condition and the same physical parameters are solved by means of the *same* mode number $N = 16384$ of the spatial Fourier expansion in $x \in [0, 2\pi]$ and the 4th-order Runge-Kutta's method, using three different time-steps, say, $\Delta t = 10^{-3}$, $\Delta t = 10^{-4}$ and $\Delta t = 10^{-5}$, respectively. Here, all physical/numerical variables and parameters are in double precision, say, $N_s = 16$. However, all of their spectrum-deviation δ_s, compared either with the CNS benchmark solution or with themself each other, increase rather quickly until beyond the reliability criteria $\delta_s^c = 1\%$ at $t \approx 175$, as shown in Fig. 6, indicating that *all* of these results given by the 4th-order Runge-Kutta's method with double precision (RKwD) have the almost *same* critical predictable time $T_c \approx 175$. This also illustrates the generality validity of the reliability criteria (25) based on the so-called spectrum-deviation (24). This is mainly because the numerical noises of the RKwD exponentially increase into the same level of the "true" solution at $t \approx 175$ so that, when $t > 175$, the numerical simulations given by the RKwD become a kind of mixture of the true solution and the numerical noises. Unfortunately, in practice a long enough interval of time is often necessary to gain a convergent statistic result. How large are the influences of the numerical noises on the chaotic simulations given by the RKwD in an interval of time longer than [0,175], such as $t \in [0, 900]$?

To investigate the influence of numerical noises on chaotic results, we compare the numerical result given by the 4th-order Runge-Kutta's method in double precision using the time-step $\Delta t = 10^{-3}$ (marked by RKwD) with the benchmark solution given by the CNS using $N = 16384$, $tol = 10^{-60}$ and $N_s = 60$ (marked by CNS). As shown in Fig. 7, the two simulations agree well at small times such as $t = 100$. As the time increases such as at $t = 200$, the numerical noises increase to such a large level that the difference between the two simulations becomes distinct. Thereafter, the numerical noises of the RKwD result increase to the same-level of the "true" solution so that the RKwD result deviates from the CNS benchmark solution larger and larger, as shown in Fig. 7(c) and (d). It means that the numerical noises rapidly propagate to the same level of the "true" chaotic solution, which lead to the great difference in spatio-temporal trajectories.

Many people believe that, for a chaotic system, the spatial energy spectrum at the time t is more fundamental than spatio-temporal trajectories. So, let us compare the spatial energy spectrums of the simulations given by the CNS and RKwD at different times. As shown in Fig. 8, at small times such as $t = 100$, the spatial energy spectrums given by the CNS and RKwD agree well with each other. However, when $t \ge 200$, their deviation of the spatial energy spectrums becomes larger and larger. For example, the relative error of c_1^2 for the 1st wave number of the spatial energy spectrum arrives 43% at $t = 200$, 289% at $t = 400$ and 6655% at $t = 600$, respectively. Especially, the even wave numbers of the

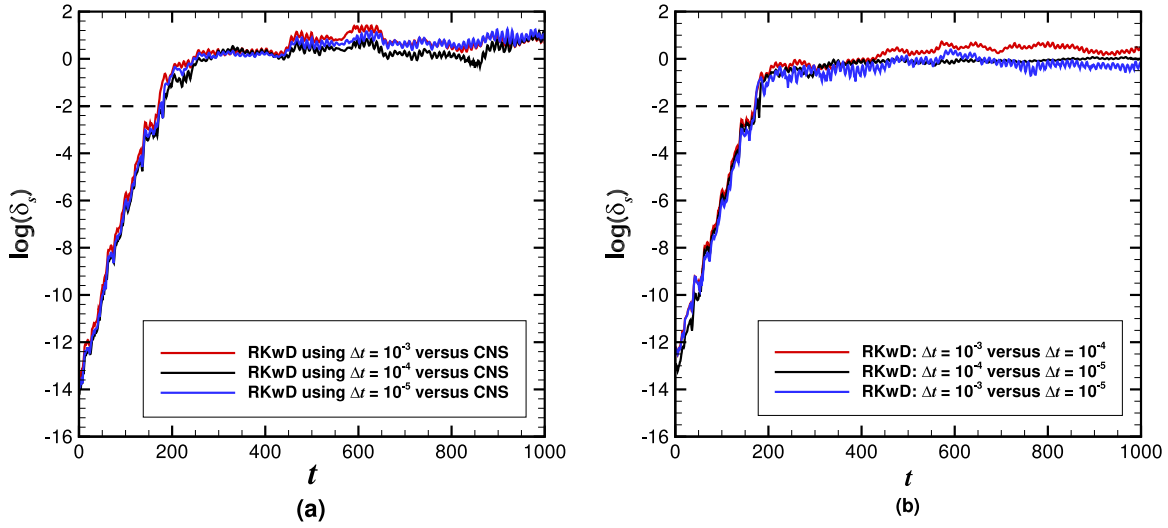

Fig. 6. Spectrum-deviation $\delta_s(t)$ of the simulations given by the 4th-order Runge-Kutta method with double precision (RKwD) using $\Delta t = 10^{-3}$, $\Delta t = 10^{-4}$ and $\Delta t = 10^{-5}$, respectively. (a) Compared with the CNS benchmark solution; (b) Compared with the RKwD simulations in different time-steps. Dashed line: $\delta_s = 1\%$.

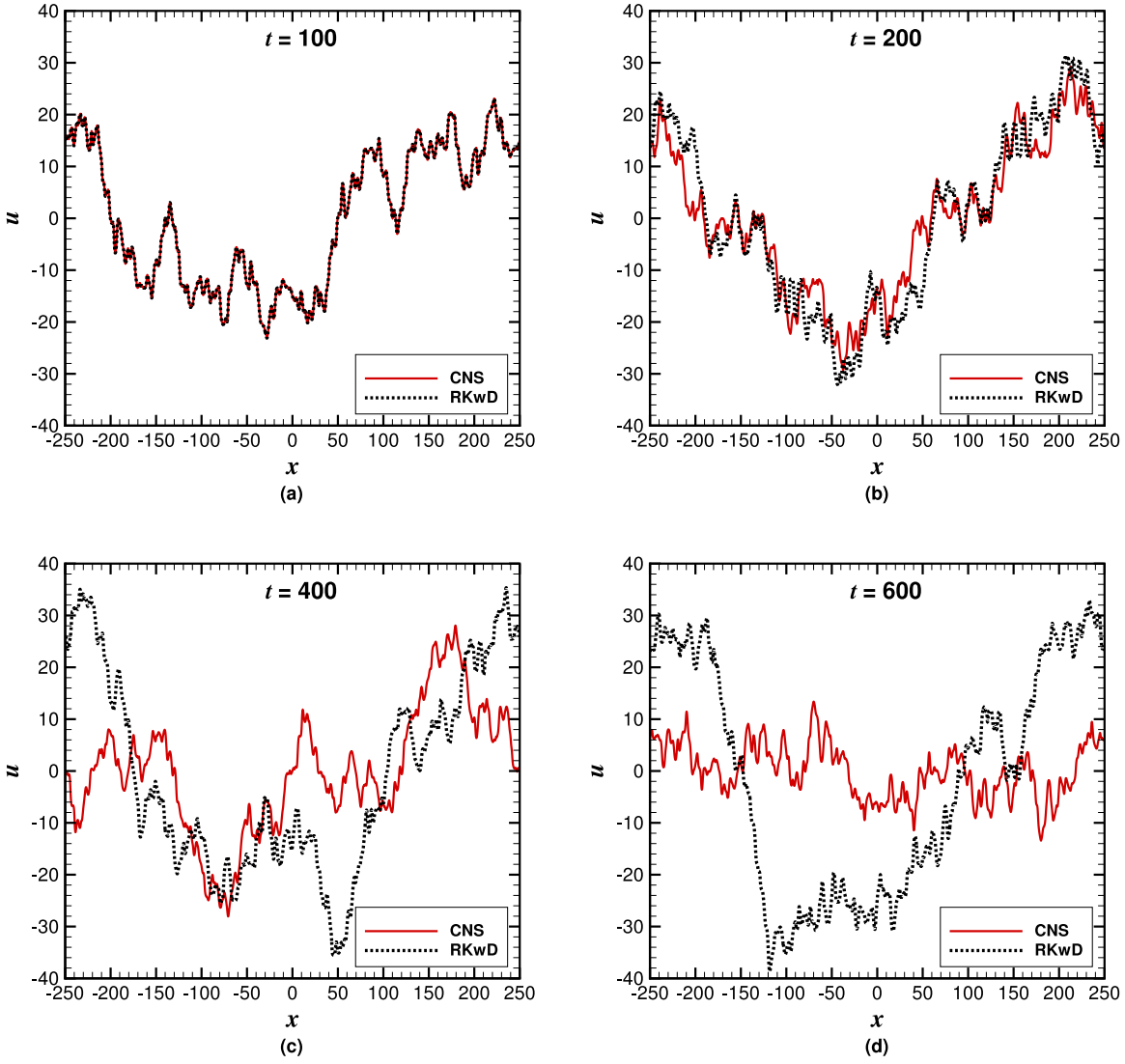

Fig. 7. Comparisons of $u(x, t)$ given by the CNS and RKwD at different times: (a) $t = 100$; (b) $t = 200$; (c) $t = 400$; (d) $t = 600$. Solid line in red: CNS benchmark result; Dashed line in black: RKwD result. (For interpretation of the references to color in this figure legend, the reader is referred to the web version of this article.)

spatial energy spectrum of the CNS benchmark solution *always* remain zero, i.e. $c_{2n} = 0$, where $n \geq 0$ is a positive integer. This reveals a kind of spatial symmetry of the true chaotic result. Surprisingly, the RKwD result gradually *losses* this kind of spatial symmetry: the even wave numbers of the spatial spectrum given by the RKwD contain no energy at $t = 100$ and small energy at $t = 200$, but thereafter more and more energy, as shown in Fig. 8(c) and (d), which finally leads to the loss of the spatial symmetry. This is unfortunately a fundamental deviation from the truth. It indicates that the random numerical noises might transfer to *all* wave numbers of the spatial spectrum at the same-level of the true solution and thus lead to large difference in spatial energy spectrum of the chaotic system, *not only* quantitatively *but also* qualitatively.

The comparison of the total spectrum energy $E_s(t) = \sum_{n=0}^{\frac{N}{2}} c_n^2(t)$ of the simulations given by the CNS and the RKwD at different times is as shown in Fig. 9(a), with the maximum relative error 2394% near $t = 619$. And the corresponding spectrum-deviation $\delta_s(t)$ is given in Fig. 9(b), with the maximum deviation 2580%. Here, it should be emphasized that the total spectrum energy $E_s(t)$ of the RKwD result might be about 24 times larger than the CNS benchmark solution! This is a huge difference. It indicates that the numerical noises might lead to huge deviation in the total energy of chaotic system.

How about the influence of numerical noises on statistical results? The comparisons of the spatial mean $\mu(t)$ and the corresponding standard deviation $\sigma(t)$ of the simulations given by the CNS and the RKwD in $0 \leq t \leq 900$ are as shown in Fig. 10(a) and (b), respectively. Note that the spatial mean $\mu(t)$ of the CNS benchmark solution *always* remains zero in the whole interval $0 \leq t \leq 900$, since the CNS result remains a kind of spatial symmetry. However, $\mu(t)$ of the RKwD simulation distinctly departs from zero when $t > 200$, with the maximum absolute error 5.35 at $t \approx 540$, mainly because the RKwD result losses the spatial symmetry when $t > 200$. Besides, when $t > 200$, the spatial standard deviation $\sigma(t)$ given by the RKwD is much larger than that of the CNS benchmark solution, with the maximum relative error 398% at $t \approx 619$. Similarly, the comparisons of the temporal mean $\mu(x)$ and the corresponding standard deviation $\sigma(x)$ of the simulations given by the CNS and the RKwD (integrated in $0 \leq t \leq 900$) are as shown in Fig. 11(a) and (b), with the maximum relative error 239% of $\mu(x)$ and 105% of $\sigma(x)$, respectively. Thus, the numerical noises might lead to huge deviations even in the *statistical* results of the spatio-temporal chaotic system.

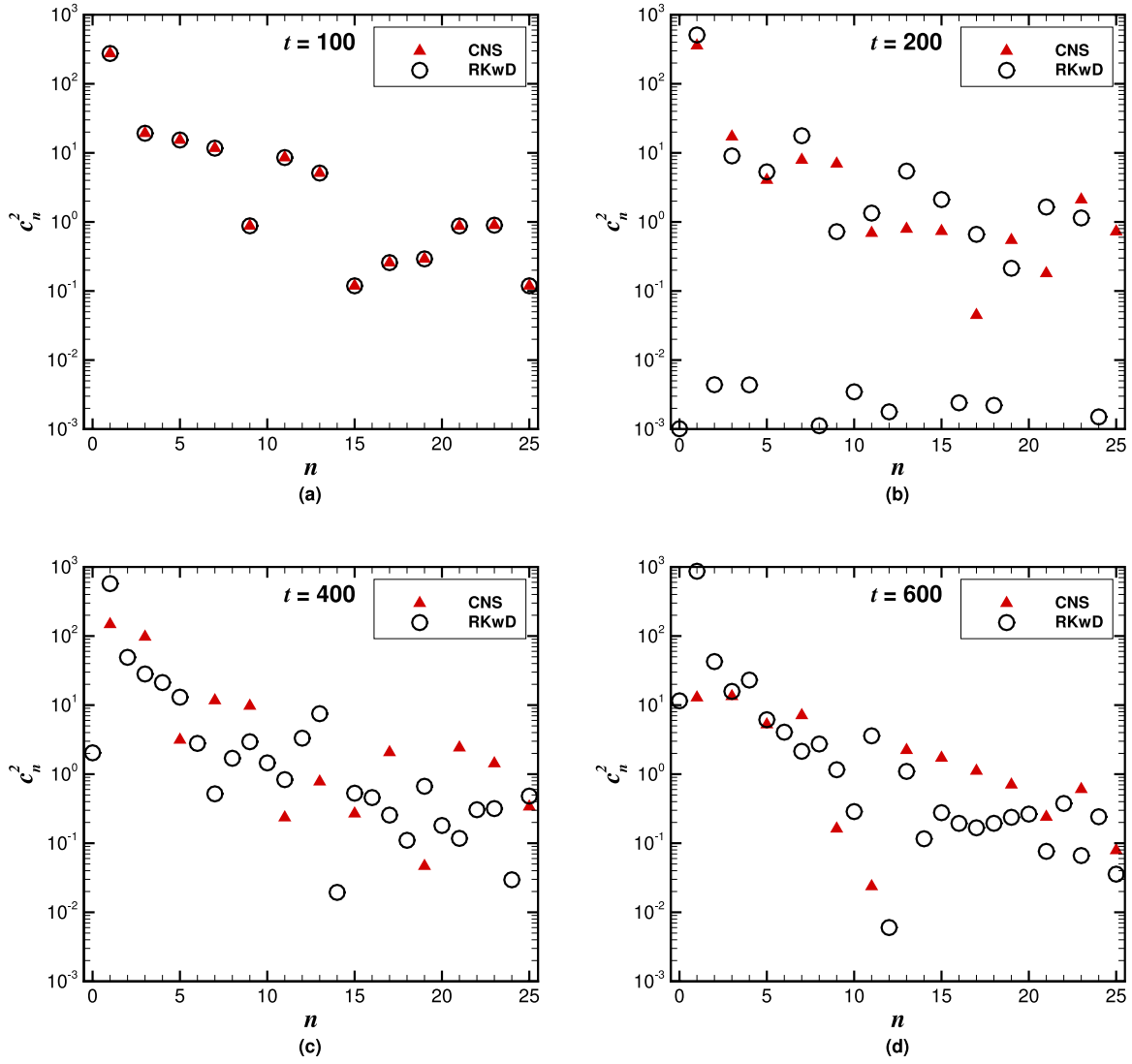

Fig. 8. Comparisons of the spatial energy spectrum given by the CNS and RKwD at different times: (a) $t = 100$; (b) $t = 200$; (c) $t = 400$; (d) $t = 600$. Triangle in red: benchmark result given by the CNS; Circle in black: result given by the RKwD. (For interpretation of the references to color in this figure legend, the reader is referred to the web version of this article.)

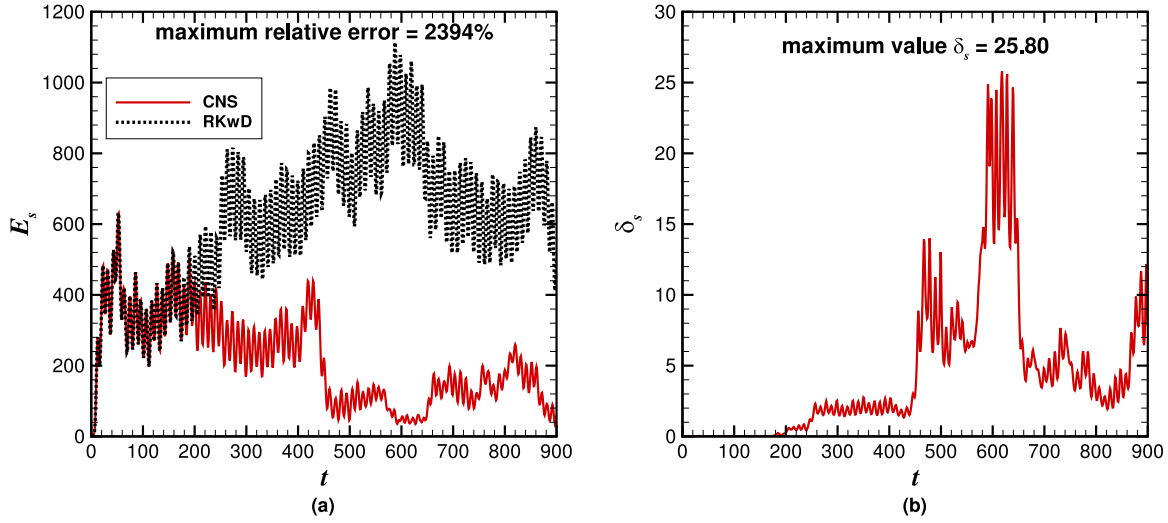

Fig. 9. (a) Comparison of the total spectrum energy $E_s(t) = \sum_{n=0}^{\frac{N}{2}} c_n^2(t)$ given by the CNS and RKwD, with the maximum relative error 2394%. Solid line in red: the CNS benchmark result; Dotted line in black: the RKwD result. (b) The corresponding spectrum-deviation $\delta_s(t)$ defined by (24), with the maximum deviation 2580%. (For interpretation of the references to color in this figure legend, the reader is referred to the web version of this article.)

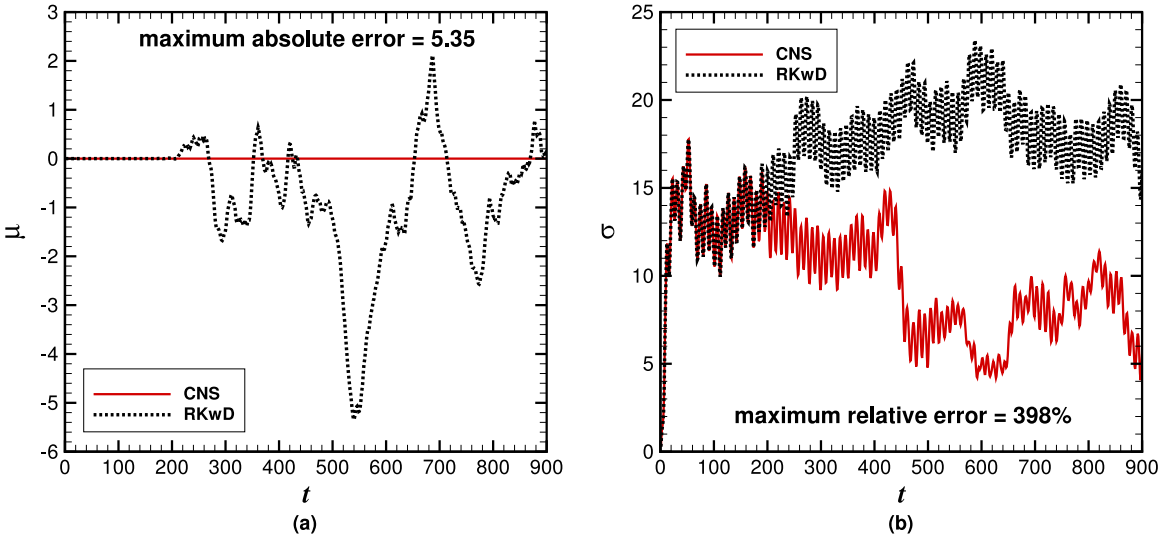

Fig. 10. Comparisons of the spatial mean $\mu(t)$ and the spatial standard deviation $\sigma(t)$ given by the CNS and RKwD in $0 \le t \le 900$, with the maximum absolute error 5.35 of $\mu(t)$ and the maximum relative error 398% of $\sigma(t)$. (a) $\mu(t)$; (b) $\sigma(t)$. Solid line in red: CNS benchmark result; Dashed line in black: RKwD result. (For interpretation of the references to color in this figure legend, the reader is referred to the web version of this article.)

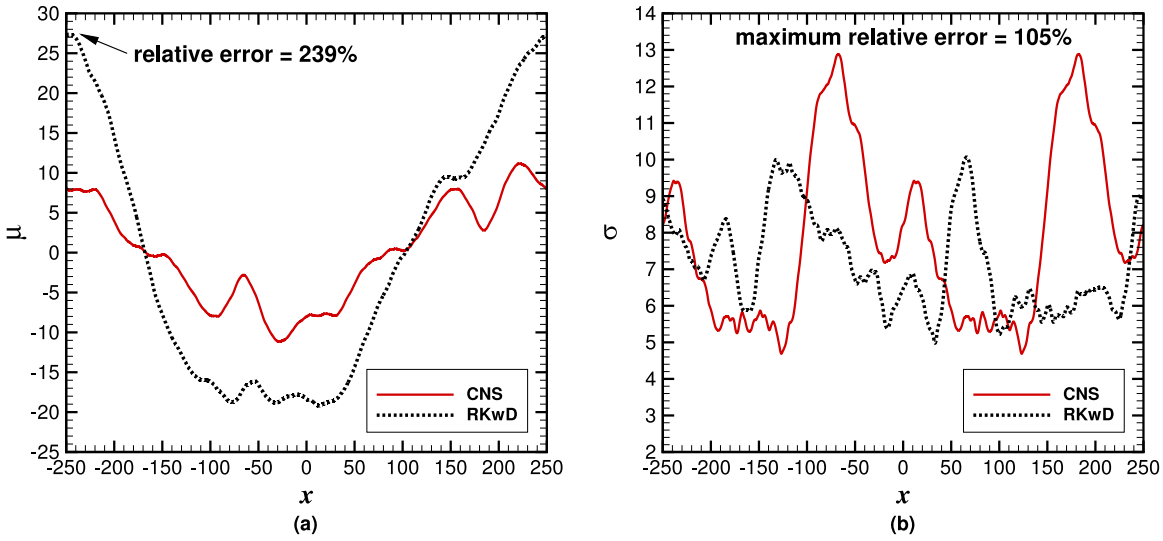

Fig. 11. Comparisons of the temporal mean $\mu(x)$ and the temporal standard deviation $\sigma(x)$ (integrated in $0 \le t \le 900$) given by the CNS and RKwD, with the maximum relative error 239% of $\mu(x)$ and 105% of $\sigma(x)$, respectively. (a) $\mu(x)$; (b) $\sigma(x)$. Solid line in red: CNS benchmark result; Dashed line in black: RKwD result. (For interpretation of the references to color in this figure legend, the reader is referred to the web version of this article.)

The comparisons of the probability density function (PDF) of the simulations given by the CNS and RKwD in different intervals of time are as shown in Fig. 12. In a short interval of time such as $0 \le t \le 200$, the PDF given by the RKwD is almost the same as that given by the CNS benchmark solution. However, as the interval of time becomes longer, the deviation of the two PDFs becomes more and more distinct. For example, the maximum relative error of the PDF for $u = 0$ is only 0.85% for the time interval $0 \le t \le 200$, but rapidly increases to 19% for $0 \le t \le 300$, 45% for $0 \le t \le 500$ and 60% for $0 \le t \le 900$, respectively. Especially, the PDFs given by the CNS benchmark solution always remains a symmetry about $u = 0$. However, the PDF given by the RKwD remains such kind of symmetry only for short intervals of time such as $0 \le t \le 200$, but thereafter gradually *losses* it, as shown in Fig. 12. This is a fundamental deviation! In addition, the PDFs given by the CNS benchmark solution are more concentrated at $u = 0$. This well explains why the result given by the RKwD contains much larger energy than that of the CNS. This indicates that the numerical noises might lead to great deviation even in the PDF of spatio-temporal chaotic system. Finally, note that the PDF given by means of the CNS result in $t \in [0, 900]$ has a distinct difference from the PDF by the CNS one in $t \in [0, 200]$, indicating that a long enough interval of time is indeed necessary for statistics.

Therefore, based on our above-mentioned comparison, the numerical noises have great influence not only on the spatio-temporal trajectories but also on the spatial spectrum, spatial symmetry, total spectrum energy and even statistical results of the chaotic system, such as the spatial/temporal mean and standard derivation as well as the probability density function (PDF).

Finally, let us consider the numerical noises

$$\mathcal{E}(x,t) = u(x,t) - u^*(x,t), \tag{29}$$

where $u(x, t)$ is the CNS benchmark solution and $u^*(x, t)$ is the RKwD simulation, respectively.

It is found that, at a large time, the numerical noises $\mathcal{E}(x,t)$ are at the same level of the RKwD simulation, as shown in Fig. 13(a) at $t = 400$ and (b) at $t = 600$. Note that the corresponding probability density functions (PDFs) of the noise $\mathcal{E}(x,t)$ at $t = 400$ and $t = 600$

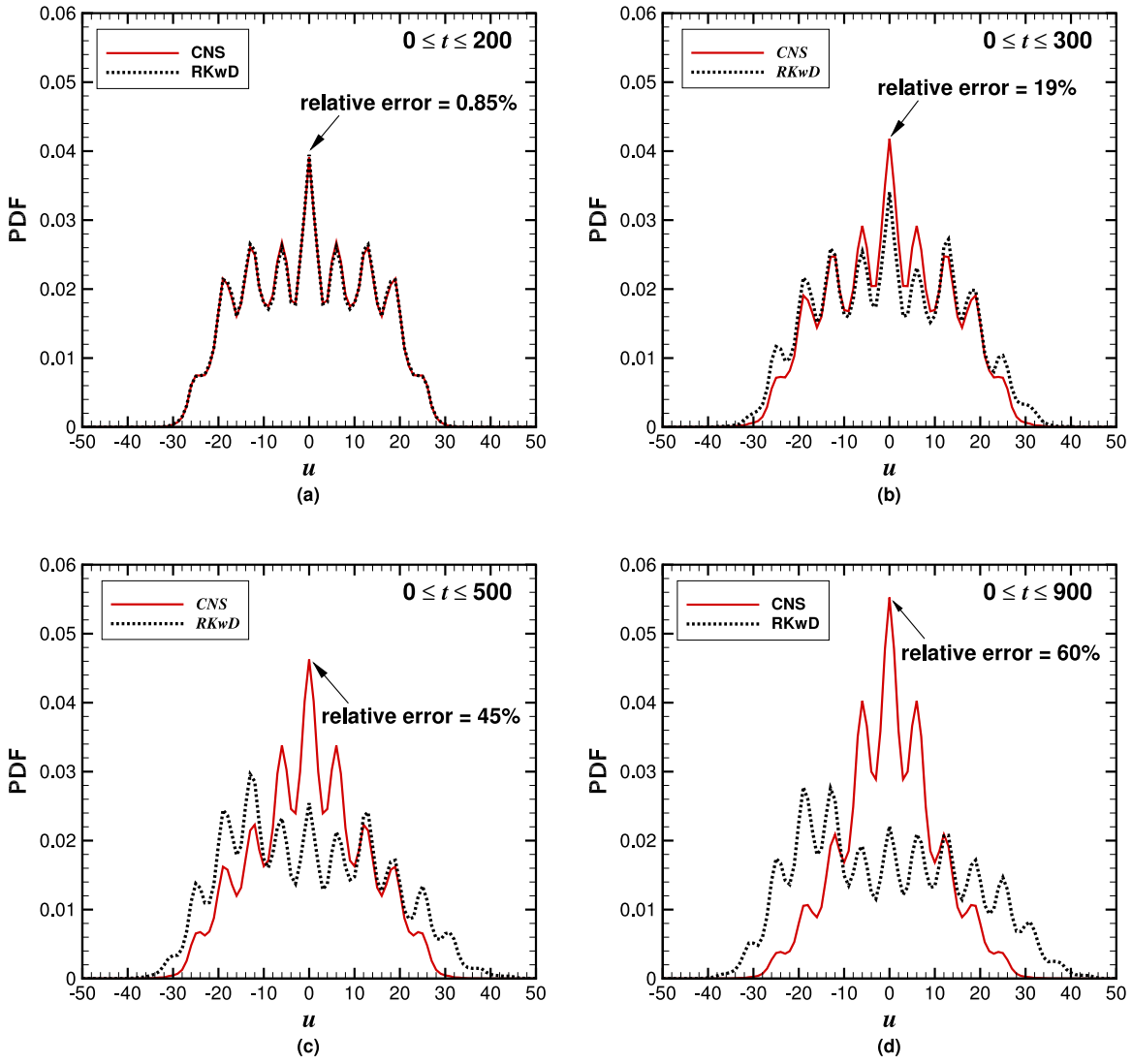

Fig. 12. Comparisons of the probability density function (PDF) of the simulations given by the CNS and RKwD in different intervals of time. (a) In $0 \le t \le 200$ with the relative error 0.85% of the PDF for $u = 0$; (b) In $0 \le t \le 300$ with the relative error 19% of the PDF for $u = 0$; (c) In $0 \le t \le 500$ with the relative error 45% of the PDF at $u = 0$; (d) In $0 \le t \le 900$ with the relative error 60% of the PDF at $u = 0$. Solid line in red: CNS benchmark result; Dashed line in black: RKwD result. (For interpretation of the references to color in this figure legend, the reader is referred to the web version of this article.)

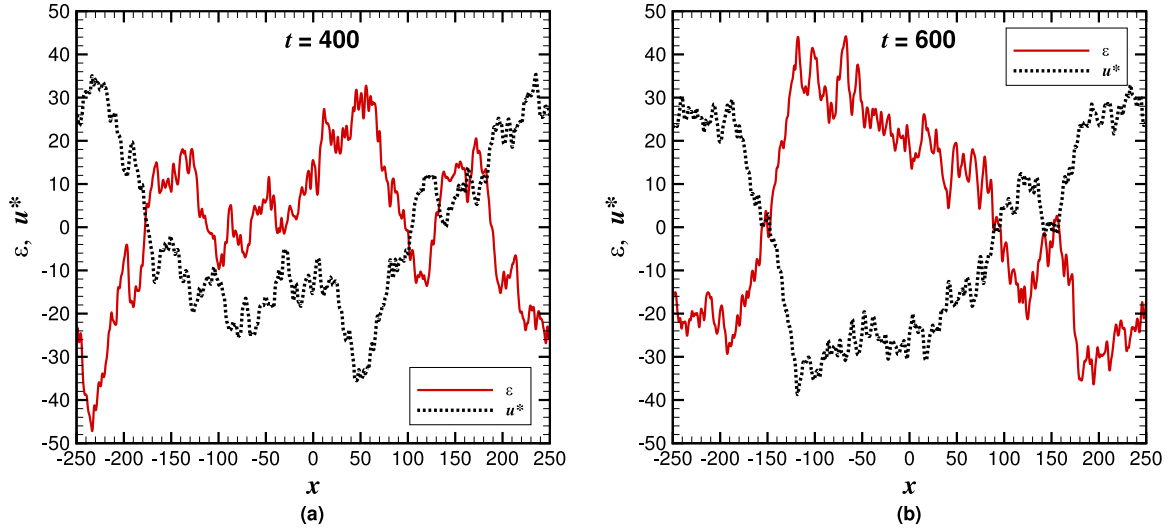

Fig. 13. Numerical noises $\mathcal{E}(x,t)$ at different time, compared with $u^*(x,t)$ given by the RKwD. (a) $t = 400$; (b) $t = 600$. Solid line in red: $\mathcal{E}(x,t)$; Dashed line in black: $u^*(x,t)$ given by the RKwD. (For interpretation of the references to color in this figure legend, the reader is referred to the web version of this article.)

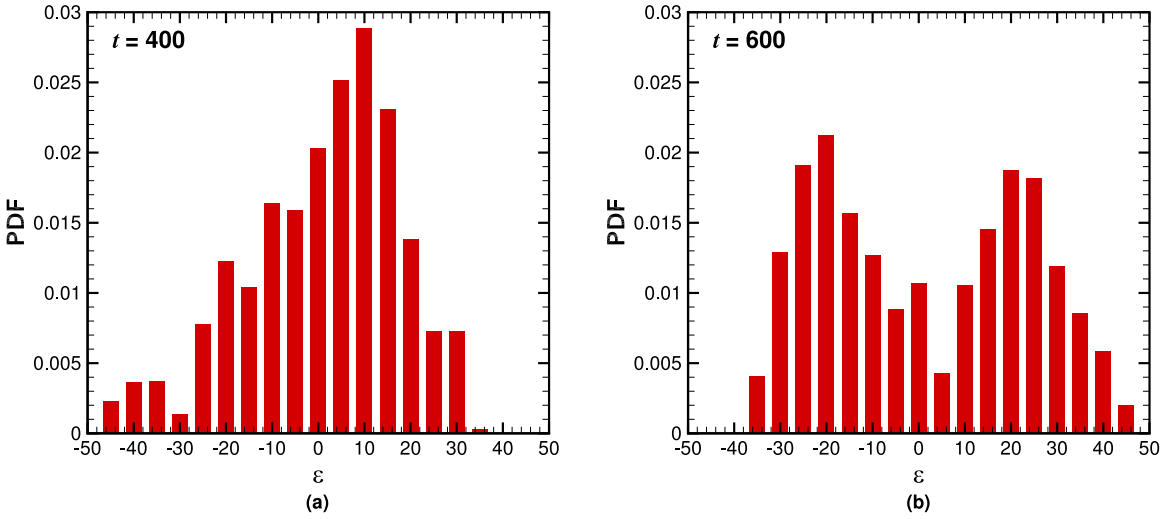

Fig. 14. PDFs of $\mathcal{E}(x,t)$ at different time. (a) $t = 400$; (b) $t = 600$.

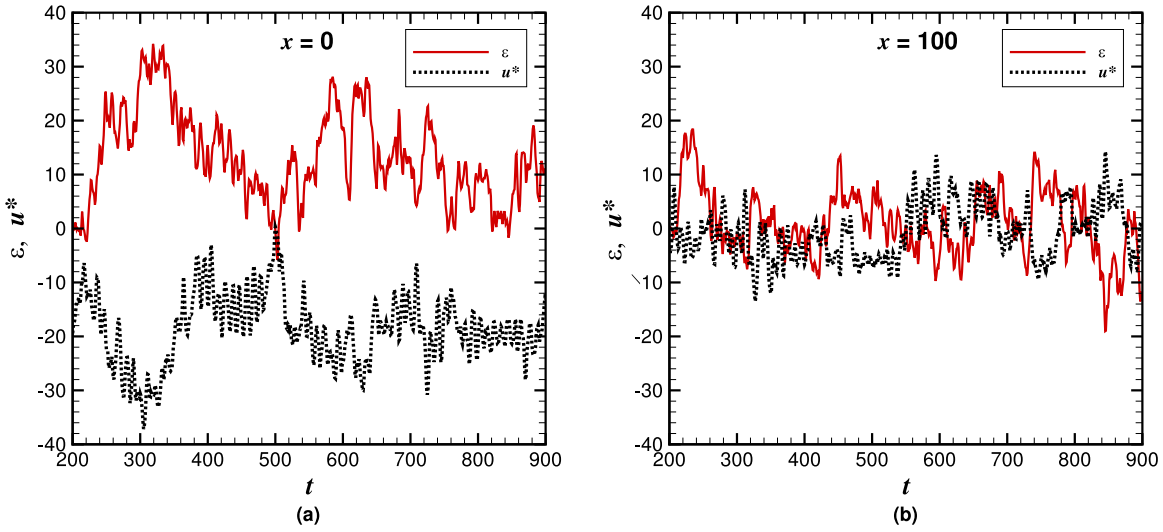

Fig. 15. Numerical noises $\mathcal{E}(x,t)$ at different spatial points, compared with $u^*(x,t)$ given by the RKwD. (a) $x = 0$; (b) $x = 100$. Solid line in red: $\mathcal{E}(x,t)$; Dashed line in black: $u^*(x,t)$ given by the RKwD. (For interpretation of the references to color in this figure legend, the reader is referred to the web version of this article.)

are time-dependent but *not* in a normal distribution, as shown in Fig. 14(a) and (b), mainly because the numerical noises are closely related to the nonlinear governing equation and thus are not independent in spatial dimension. Similarly, $\mathcal{E}(x,t)$ in temporal dimension ($t \geq 200$) are also at the same level of the simulation given by the RKwD, as shown in Fig. 15(a) at $x = 0$ and (b) at $x = 100$, respectively. Besides, their PDFs are also *not* in a normal distribution, as shown in Fig. 16(a) and (b).

It should be emphasized that, after a long enough time, the numerical noise $\mathcal{E}(x,t)$ is at the *same* level of the RKwD simulation, and besides the probability density functions of the noise $\mathcal{E}(x,t)$ are *not* in a normal distribution in both of temporal and spatial dimensions. These explain why the numerical noises have great influence on numerical simulations of spatio-temporal chaos given by traditional algorithms in double precision, not only *quantitatively* but also *qualitatively*. It also confirms the hypothesis that numerical noise increases exponentially.

Spatio-temporal chaotic systems widely exist in science and engineering, which are however solved by traditional algorithms mostly in double precision. Besides, from the viewpoint of statistics, a long-duration numerical simulation is often necessary in practice. However, as illustrated above, numerical simulations gained in the traditional way might be wrong even in statistics. Obviously, these wrong statistical results might mislead us and hinder our better understanding on these chaotic systems. The new strategy of the CNS in physical space provides us an efficient way to more accurately study lots of spatio-temporal chaotic systems in science, finance and engineering in a long enough interval of time so as to reveal some new physical truths by means of clearing away numerical noises.

5. Conclusion

Due to the famous butterfly-effect of chaos, computer-generated simulations often depart quickly from true solution of a chaotic system. According to Anosov [12] and Bowen [13], *uniformly hyperbolic* systems have the so-called shadowing property, say, a computer-generated trajectory will stay close to (shadow) true trajectories with *adjusted* initial conditions for arbitrarily long times [12–17]. However, *hardly* any of chaotic systems is uniformly hyperbolic. Thus, the good promise from the Shadow Lemma [12,13] does not work on many non-hyperbolic systems [21].

In this paper, a strategy of the Clean Numerical Simulation (CNS) in physical space is proposed to efficiently gain

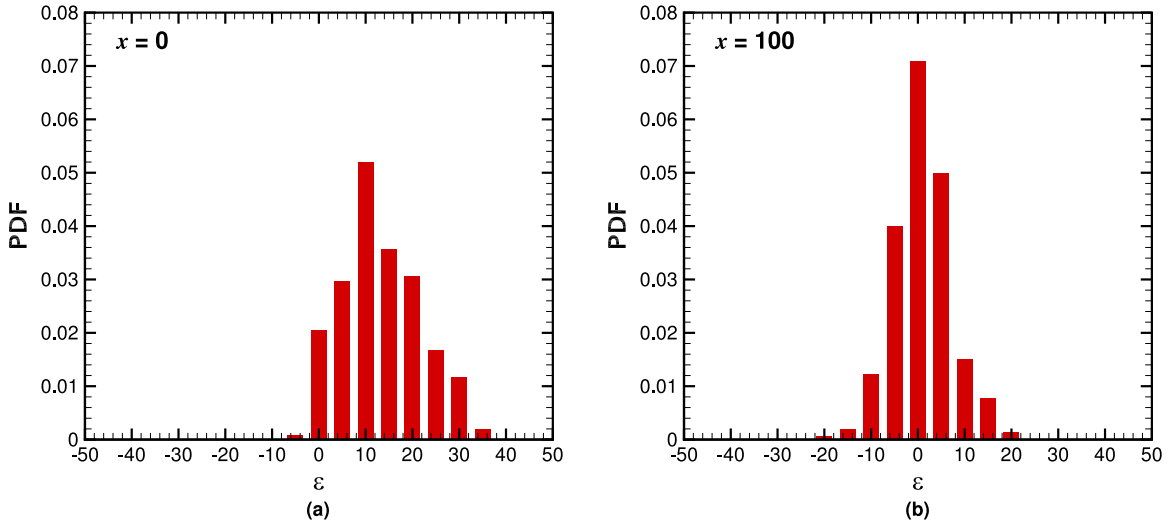

Fig. 16. PDFs of $\mathcal{E}(x,t)$ (in $200 \le t \le 900$) at different spatial points. (a) $x = 0$; (b) $x = 100$.

reliable/convergent computer-generated simulations of spatio-temporal chaotic systems. This CNS algorithm reduces both of truncation error and round-off error to such a required tiny level that the corresponding numerical simulation is reliable in an interval of time $t \in [0, T_c]$ within the total spatial domain. In practice, the value of the so-called critical predictable time T_c is determined by comparing this simulation with an additional one (in the same case) given by the CNS using even smaller numerical noises, so that both of them has no distinct differences in $t \in [0, T_c]$. Unlike the Shadow Lemma [12,13], this CNS algorithm is valid even for non-hyperbolic systems and thus is more general.

In this paper the damped driven sine-Gordon equation is used as an example to illustrate the validity of this CNS algorithm in physical space for spatio-temporal chaos. A reliable numerical simulation is obtained by this CNS algorithm in a long enough interval of time $0 \le t \le 900$, which is then used as a benchmark solution to investigate the influence of numerical noises by comparing it with those given by the traditional Runge-Kutta's method in double precision. It is found that numerical noise can lead to, both quantitatively and qualitatively, huge deviation of the spatio-temporal chaotic system not only in trajectories but also even in *statistics*! Therefore, we should check very carefully the reliability of computer-generated simulations of spatio-temporal chaotic systems (including turbulent flows), especially when the duration of simulation is quite long.

Spatio-temporal chaotic systems widely exist in science and engineering, which are however solved by traditional algorithms mostly in double precision. Besides, from the viewpoint of statistics, a long-duration numerical simulation is often necessary in practice. However, as illustrated above, numerical simulations gained in the traditional way might be wrong even in statistics. Obviously, these wrong statistical results might mislead us and hinder our better understanding on these chaotic systems. The new strategy of the CNS algorithm in physical space provides us a more efficient way to gain reliable computer-generated simulation of spatio-temporal chaos in a long enough interval of time so as to reveal some new physical truths by means of clearing away numerical noises. Such kind of clean, reliable simulations in a long enough duration of time certain could have many important applications in science and engineering. For example, "clean" numerical simulations of turbulent flows might reveal more accurately some physical truths and essences of turbulence. Hopefully, the CNS could bring us more accurate and more reliable computer-generated simulations for many complicated chaotic problems, such as three-body problem, quantum chaos, turbulence and so on, so as to greatly deepen our understandings and enrich our knowledge about them.

Declaration of Competing Interest

The authors declare that they have no known competing financial interests or personal relationships that could have appeared to influence the work reported in this paper.

CRediT authorship contribution statement

Shijie Qin: Software, Data curation, Methodology, Writing - original draft. **Shijun Liao:** Conceptualization, Methodology, Writing - original draft, Supervision, Funding acquisition.

Acknowledgment

Thanks to the anonymous reviewers for their valuable comments and suggestions. This work is supported by the National Natural Science Foundation of China (No. 91752104).

References

[1] Li TY, Yorke JA. Period three implies chaos. Am Math Mon 1975;82(10):985–92.
[2] Lorenz EN. The essence of chaos. University of Washington Press; 1993.
[3] Parker TS, Chua LO. Practical numerical algorithms for chaotic systems. Math Comput 1989;66(1):125–8.
[4] Peter S. Explaining chaos. Cambridge University Press; 1998.
[5] Sprott JC. Elegant chaos: algebraically simple chaotic flows. Singapore: World Scientific; 2010.
[6] Altan A, Karasu S, Bekiros S. Digital currency forecasting with chaotic meta-heuristic bio-inspired signal processing techniques. Chaos Solitons Fractals 2019;126:325–36.
[7] Poincaré JH. Sur le probléme des trois corps et les équations de la dynamique. Divergence des séries de m. Lindstedt. Acta Math 1890;13:1–270.
[8] Lorenz EN. Deterministic nonperiodic flow. J Atmos Sci 1963;20(2):130–41.
[9] Sprott JC. Chaos and time-series analysis. Oxford University Press; 2003.
[10] Lorenz EN. Computational periodicity as observed in a simple system. Tellus Ser A 2006;58(5):549–57.
[11] Teixeira J, Reynolds CA, Judd K. Time step sensitivity of nonlinear atmospheric models: numerical convergence, truncation error growth, and ensemble design. J Atmos Sci 2007;64(1):175.
[12] Anosov DV. Geodesic flows and closed Riemannian manifolds with negative curvature. Proc Steklov Inst Math 1967;90:3–210.
[13] Bowen R. ω-limit sets for Axiom A diffeomorphisms. J Differ Equ 1975;18:333–9.
[14] Hammel SM, Yorke JA, Grebogi C. Do numerical orbits of chaotic dynamical processes represent true orbits? J Complex 1987;3(2):136–45.
[15] Hammel SM, Yorke JA, Grebogi C. Numerical orbits of chaotic processes represent true orbits. Bull Am Math Soc 1988;19(2):465–9.

[16] Grebogi C, Hammel SM, Yorke JA, Sauer T. Shadowing of physical trajectories in chaotic dynamics: containment and refinement. Phys Rev Lett 1990;65(13):1527.
[17] Sauer T, Yorke JA. Rigorous verification of trajectories for the computer simulation of dynamical systems. Nonlinearity 1991;4(3):961.
[18] Dawson S, Grebogi C, Sauer T, Yorke JA. Obstructions to shadowing when a Lyapunov exponent fluctuates about zero. Phys Rev Lett 1994;73(14):1927.
[19] Do Y, Lai Y-C. Statistics of shadowing time in nonhyperbolic chaotic systems with unstable dimension variability. Phys Rev E 2004;69(1):016213.
[20] Sauer TD. Shadowing breakdown and large errors in dynamical simulations of physical systems. Phys Rev E 2002;65(3):036220.
[21] Anishchenko V, Kopeikin A, Kurths J, Vadivasova T, Strelkova G. Studying hyperbolicity in chaotic systems. Phys Lett A 2000;270:301.
[22] Hayes WB, Jackson KR. A fast shadowing algorithm for high-dimensional ODE systems. SIAM J Sci Comput 2007;29(4):1738–58.
[23] Liao S. On the reliability of computed chaotic solutions of non-linear differential equations. Tellus A 2009;61(4):550–64.
[24] Liao S. On the numerical simulation of propagation of micro-level inherent uncertainty for chaotic dynamic systems. Chaos Solitons Fractals 2013;47:1–12.
[25] Liao S. Physical limit of prediction for chaotic motion of three-body problem. Commun Nonlinear Sci Numer Simul 2014;19(3):601–16.
[26] Corliss G, Chang YF. Solving ordinary differential equations using taylor series. ACM Trans Math Softw 1982;8(2):114–44.
[27] Oyanarte P. MP-A multiple precision package. Comput Phys Commun 1990;59(2):345–58.
[28] Liao S, Wang P. On the mathematically reliable long-term simulation of chaotic solutions of lorenz equation in the interval [0, 10000]. Sci China Phys Mech Astron 2014;57(2):330–5.
[29] Lin Z, Wang L, Liao S. On the origin of intrinsic randomness of Rayleigh–Bénard turbulence. Sci China Phys Mech Astron 2017;60(1):14712.
[30] Li X, Liao S. More than six hundred new families of newtonian periodic planar collisionless three-body orbits. Sci China Phys Mech Astron 2017;60(12):129511.
[31] Li X, Yipeng J, Shijun L. Over a thousand new periodic orbits of a planar three--body system with unequal masses. Publ Astron Soc Jpn 2018;0(0):1–7.
[32] Li X, Liao S. Collisionless periodic orbits in the free-fall three-body problem. New Astron 2019;70:22–6.
[33] Crane L. Infamous three-body problem has over a thousand new solutions. New Scientist 2017. New Scientist, 20 September 2017, (https://www.newscientist.com/article/2148074-infamous-three-body-problem-has-over-a-thousand-new-solutions/)
[34] Whyte C. Watch the weird new solutions to the baffling three-body problem. New Scientist 2018. New Scientists, 25 May 2018, (https://www.newscientist.com/article/2170161-watch-the-weird-new-solutions-to-the-baffling-three-body-problem/)
[35] Aranson I, Levine H, Tsimring L. Controlling spatiotemporal chaos. Phys Rev Lett 1994;72(16):2561.
[36] Chacón R, Bellorín A, Guerrero L, González J. Spatiotemporal chaos in sine–Gordon systems subjected to wave fields: onset and suppression. Phys Rev E 2008;77(4):46212.
[37] Keller JB, Mclaughlin DW, Papanicolaou GC. Surveys in applied mathematics. Plenum Press; 1995.
[38] Ferré MA, Clerc MG, Coulibally S, Rojas RG, Tlidi M. Localized structures and spatiotemporal chaos: comparison between the driven damped sine-Gordon and the Lugiato-Lefever model. Eur Phys J D 2017;71(6):172.
[39] Barrio R, Blesa F, Lara M. VSVO formulation of the Taylor method for the numerical solution of ODEs. Comput Math Appl 2005;50(1):93–111.